4. T. Geiger and S. Clarke, *J. Biol. Chem.* **262**, 785 (1987); S. Clarke, *Ann. Rev. Biochem.* **54**, 479 (1985).
5. B. A. Johnson and D. W. Aswad, *Biochemistry* **24**, 2581 (1985).
6. A. B. Robinson, J. H. McKerrow, P. Cary, *Proc. Natl. Acad. Sci. U.S.A.* **66**, 753 (1970).
7. E. D. Murray and S. Clarke, *J. Biol. Chem.* **258**, 10722 (1983); P. Bornstein and G. Balian, *Methods Enzymol.* **47**, 132 (1977); Y. C. Meinwald, E. R. Stinson, H. A. Scheraga, *Int. J. Peptide Protein Res.* **28**, 79 (1986).
8. It was not determined whether deamidation of the groups occurred prior to crystallization or during the period of crystal growth and data collection. Trypsin crystals grown to neutron size (4 mm^3) took approximately 1 year; subsequent soaking in D_2O and data collection took an additional 6 months. It is not expected that D_2O would greatly influence the deamidation process; analysis of the H_2O trypsin structure showed similar deamidation traits.
9. Experimental procedures are described in A. A. Kossiakoff and S. A. Spencer, *Biochemistry* **20**, 6462 (1981).
10. A fermi is a measure of the scattering capacity of a type of atom (such as hydrogen, nitrogen, or oxygen) toward neutrons and is similar to an x-ray form factor. Fermis are in units of scattering length, 10^{-13} cm.
11. Temperature factors measure the inherent vibratory motion of an atom defined as $B = 8\pi^2 \langle U^2 \rangle$ Å^2, where $\langle U^2 \rangle$ is the mean squared amplitude of atomic vibration.
12. J. Shpungin and A. A. Kossiakoff, *Methods Enzymol.* **127**, 329 (1986).
13. Integrated intensities at the Nδ2 deuterium sites of residues 48 and 95 were less than 10% the expected value for a fully exchanged site; for Asn^{115}, the densities were about 25% those of a full site.
14. J. S. Richardson, *Adv. Protein Chem.* **34**, 167 (1981).
15. $X1$ is a torsion angle defining the angular rotation of the hydroxyl group around the Cα–Cβ bond.
16. D. W. Aswad, *J. Biol. Chem.* **259**, 10714 (1984); B. A. Johnson, E. D. Murray, S. Clarke, D. B. Glass, D. W. Aswad, *ibid.* **262**, 5622 (1987).
17. The author acknowledges the technical assistance of J. Shpungin and thanks B. Schoenborn and his colleagues, who developed the neutron diffraction station at the Brookhaven High Flux Beam Reactor, and R. Wetzel for his suggestions during preparation of the manuscript.

16 November 1987; accepted 18 February 1988

Electric Field X-ray Scattering Measurements on Tobacco Mosaic Virus

M. H. J. Koch, E. Dorrington, R. Kläring, A. M. Michon, Z. Sayers, R. Marquet, C. Houssier

The feasibility of electric field x-ray solution scattering with biological macromolecules was investigated. Electric field pulses (1.25 to 5.5 kilovolts per centimeter) were used to orient tobacco mosaic virus in solution (4.5 milligrams per milliliter). The x-ray scattering is characteristic of isolated oriented particles. The molecular orientation and its field-free decay were monitored with a time resolution of 2 milliseconds by means of synchrotron radiation and a multiwire proportional area detector. The method should also be applicable to synthetic polymers and inorganic colloids.

It has been known at least since the beginning of the century (*1*) that electric fields affect light scattering. Light scattering in the presence of electric fields has been used to obtain information on a variety of materials ranging from viruses and nucleic acids to synthetic polymers and clays [for a review, see (*2*)]. Full use of the method requires particles sufficiently large, or a wavelength sufficiently short, for the scattering to be influenced by internal interference effects. The small ratio of particle size to wavelength and the strong absorption by samples are usually the limiting factors in electric field light scattering. These limitations can in principle be overcome by using x-rays.

X-ray electric field scattering should have two advantages, the first being the ability to study the effects of electric fields on macromolecules, thus bridging the gap between structural and electrooptical methods [for an introduction, see (*3*)]. The second would be the possibility of obtaining at least transiently, even with dilute systems, a partially oriented scattering pattern. It is mainly this second possibility that prompted us to perform the feasibility experiments described below, because there is some advantage in the study of fibrous systems like chromatin (*4*) in being able to unequivocally assign specific features of the solution scattering patterns to meridional or equatorial contributions in the pattern of oriented specimens. As an obvious test object for these experiments we chose tobacco mosaic virus (TMV), which is perhaps the system most thoroughly studied by electric dichroism and birefringence (*5–8*) and electric field light scattering (*9*). Furthermore, magnetic field orientation methods (*10, 11*) have been used on very concentrated TMV samples that display liquid crystalline behavior.

The x-ray scattering measurements were carried out on the X33 camera of the European Molecular Biology Laboratory (EMBL) in the Hamburg Synchrotron Laboratory (HASYLAB) (*12*) on the storage ring DORIS of the Deutsches Elektronen Synchrotron (DESY) at Hamburg.

The solution of TMV (4.5 mg/ml) in a buffer with 0.3 m*M* NaCl, 0.2 mM tris-HCl (*p*H 7.5), 3 m*M* EDTA, and 0.5 m*M* phenylmethylsulfonyl fluoride (PMSF) was contained in a cell with platinum electrodes (*13*). Electric field pulses (1.25 to 5.25 kV/cm) produced by a power pulse generator triggered by the data acquisition system (*14, 15*) were applied to the electrodes of the measurement cell. Two types of multiwire proportional detectors with delay-line readout (*16*) were used. The first is a quadrant detector (*17*) that integrates the scattering pattern azimuthally in one quadrant. This detector was placed alternately with the bisector of the quadrant along the field and perpendicular to the field and used to collect sequences of 128 time frames of 2 msec each. The second is an area detector with 256 by 256 elements, a resolution of 1 mm, and a dead time of 470 nsec (*18*).

Unipolar pulses were applied for 2 msec and the polarity was reversed before each new pulse. X-ray scattering data were accumulated for a series of 20 pulses, processed, and checked for degradation of the response of the sample. Damage to the samples could largely be eliminated by using bipolar pulses and a fast shutter to protect the samples from radiation between measurements. The same data acquisition system can be used for optical measurements (*19*).

Figure 1A illustrates the x-ray solution scattering pattern of a TMV solution under normal conditions. The shape of the scattering curves at low angle indicates that, under the conditions used, there is some polydispersity, but the contribution of side by side aggregates amounts to only a few percent of the scattered intensity. Figure 1B results from the accumulation of 200 pulses of 2 msec duration with an applied electric field of 5 kV/cm. The relative differences ($\Delta I/I$) resulting from the applied field shown in Fig. 1C indicate a decrease of the scattered intensity by about 40% in the direction parallel to the field and a corresponding increase in the direction perpendicular to the field. This result indicates that in the region of saturation, at high fields, all particles are indeed oriented and illustrates the identity between the electrooptical orientation parameter and the structural order parameter. Note that Fig. 1B corresponds to the continuous transform of an isolated, oriented particle. It is thus different from the pattern of an oriented gel, where the transform is

M. H. J. Koch, E. Dorrington, R. Kläring, A. M. Michon, Z. Sayers, European Molecular Biology Laboratory, c/o DESY, D-2000 Hamburg 52, Federal Republic of Germany.
R. Marquet and C. Houssier, Laboratoire de Chimie Macromoléculaire et Chimie Physique, Sart Tilman, Université de Liège, B-4000 Liège, Belgium.

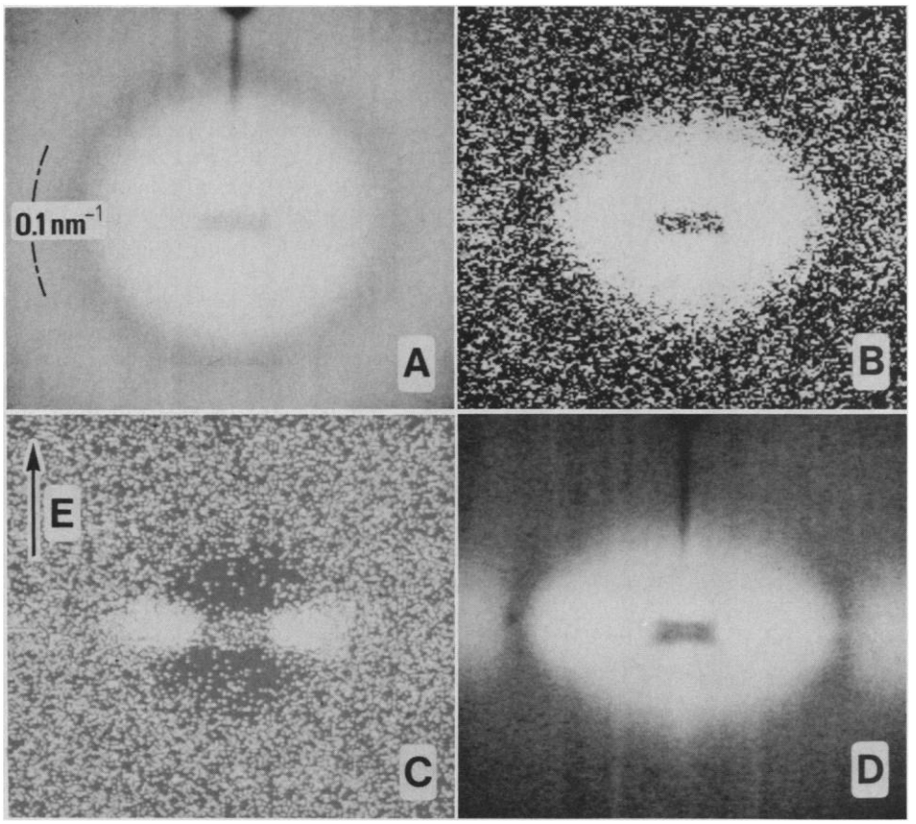

Fig. 1. (**A**) Area-detector small-angle x-ray scattering patterns from a solution of TMV (4.5 mg/ml). (**B**) Pattern from the same solution during the application of an electric field of 5 kV/cm. (**C**) Relative differences [(B − A)/A] in the pattern upon application of the electric field. The arrow labeled E indicates the direction of the electric field. (**D**) Pattern of an oriented gel of TMV. The detector covers the range of scattering vectors $0.01 \leq s \leq 0.15$ nm^{-1} as indicated in (A).

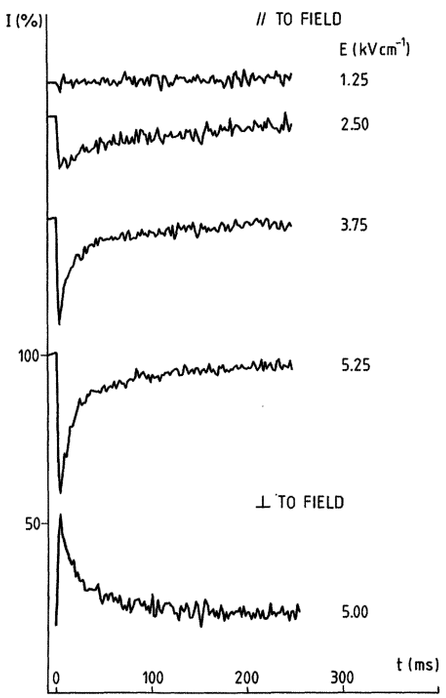

Fig. 2. Time course of the relative difference along the direction of the applied field (meridian) and perpendicular to it (equator) at different field strengths. The curves are shifted for better visualization. Intensity in absence of field is 100% for all curves.

sampled by a lattice. The pattern of an oriented TMV gel is shown for comparison in Fig. 1D. The time courses of the intensities integrated in the range of scattering vectors $0.01 \leq s \leq 0.1$ nm^{-1} (where $s = 2 \sin \theta/\lambda$, 2θ is the scattering angle, and λ the wavelength) in the directions parallel and perpendicular to the field at different field strengths are illustrated in Fig. 2. These curves correspond to field-free relaxation. The results of the optical measurements (not shown) made with the alternative experimental arrangement indicate that under identical conditions of *p*H and concentrations one obtains the same relaxation curves as with x-ray scattering. This is expected, as both scattering and birefringence yield a signal that depends on the weight average of the components.

The polydispersity of the sample explains the shape of the relaxation curves. Polydispersity is also observed in dilute solutions at *p*H values below 8.2 and appears to be due to the formation of end to end dimers (*8*). At lower field values only the larger aggregates orient and give rise to the slow relaxation component.

The fields required to obtain orientation and its saturation are much higher than in dilute solutions, where a few hundred volts per centimeter suffice. This is because at higher concentrations the effective field seen by the individual particles is strongly reduced by the polarization of the medium (*8*). The relaxation time of the fastest component detected here is 8 msec. This value is obtained by a peeling method analogous to that used for electrooptical data (*20*). The curve at 2.5 kV/cm, which corresponds essentially to the orientation of large aggregates, yields a relaxation time of about 120 msec.

Electrooptical methods in dilute solution (≤1 mg/ml) (*7, 8*) give relaxation times of 500 μsec for the monomer and about 2 msec for end to end dimers. Analysis of the effect of end to end polymerization on the relaxation rate (*20*) indicates that the higher value observed here can be accounted for by assuming that it is mainly the relaxation of end to end dimers and trimers that is observed. This has been confirmed by electron microscopic observations on similar samples. Note, however, that end to end polymerization does not affect the shape of the scattering patterns in Fig. 1.

The scattering patterns in Fig. 1 give a direct proof that electric dichroism in dilute solutions is indeed the result of the transient orientation of the TMV particles with their axis parallel to the field. In the case of TMV this orientation had been inferred from the positive flow birefringence (*21*) and electric-field birefringence (*6*). Electric field x-ray scattering should allow us to relate more directly the orientation with that of the field in systems where the directions of the induced or permanent dipoles are less obvious.

For static x-ray scattering measurements on concentrated samples with liquid crystalline behavior magnetic fields are probably easier to use than the present method [for a review, see (*22*)]. The advantage of electric fields is that a large number of systems can be oriented even in dilute solution and relaxation times can be measured. Our results indicate that there is potential for development of this method, which has in principle a wide range of applications. One of the main challenges is obviously the further development of high-efficiency area x-ray detectors with rapid framing.

REFERENCES AND NOTES

1. E. Bloch, *Compt. Rend. Acad. Sci.* **146**, 971 (1907).
2. B. R. Jennings, in *Molecular Electro-optics*, part 1, *Theory and Methods*, C. T. O'Konski, Ed. (Dekker, New York, 1976), pp. 275–319.
3. E. Fredericq and C. Houssier, *Electric Dichroism and Electric Birefringence* (Clarendon, Oxford, 1973).
4. M. H. J. Koch *et al.*, *Eur. J. Biophys.* **15**, 133 (1987).
5. H. Benoit, *J. Chim. Phys. Phys. Chim. Biol.* **47**, 719 (1950).

6. C. T. O'Konski and B. H. Zimm, *Science* **111**, 113 (1950).
7. C. T. O'Konski and A. J. Haltner, *J. Am. Chem. Soc.* **79**, 5634 (1957).
8. F. S. Allen and K. E. Van Holde, *Biopolymers* **10**, 865 (1976).
9. B. R. Jennings and H. G. Jerrard, *J. Chem. Phys.* **44**, 1291 (1966).
10. S. Fraden, A. J. Hurd, R. B. Meyer, M. Cahoon, D. L. D. Caspar, *J. Phys.* **46**, C385 (1985).
11. R. Oldenbourg and W. C. Phillips, *Rev. Sci. Instrum.* **57**, 2362 (1986).
12. M. H. J. Koch and J. Bordas, *Nucl. Instrum. Methods* **208**, 461 (1983).
13. The geometry of the cell is identical to that used for conventional solution scattering experiments without field. Its thickness (1 mm) is imposed by the optimal thickness of aqueous solutions at a wavelength of 0.15 nm, and its width (7 mm) by the maximum cross section of the x-ray beam at the sample position. The platinum electrodes forming the top and bottom walls of the cell are separated by 4 mm. The resistance of the cell when filled with distilled water is about 1 megohm. The windows consist of 15-μm-thick mica.
14. C. Boulin *et al.*, *Nucl. Instrum. Methods* **201**, 209 (1982).
15. C. Boulin *et al.*, *ibid.* **A249**, 399 (1986).
16. A. Gabriel and F. Dauvergne, *ibid.* **201**, 223 (1982).
17. J. Hendrix, A. Gabriel, C. Boulin, unpublished.
18. A. Gabriel, C. Boulin, M. H. J. Koch, *Nucl. Instrum. Methods*, in press.
19. A helium-neon laser is used as source of polarized light and the mica windows of the cell are replaced by quartz.
20. C. T. O'Konski and A. J. Haltner, *J. Am. Chem. Soc.* **78**, 3604 (1956).
21. M. A. Lauffer, *J. Phys. Chem.* **42**, 935 (1938).
22. J. Torbet, *Trends Biochem. Sci.* **12**, 327 (1987).
23. We thank J. Witz (IBMC-Strasbourg) for his gift of the TMV sample, E. Mandelkow for the oriented fiber, H. J. Brosch (MKI, DESY) for lending us the Cober generator, and D. J. Thompson (SERC Daresbury Laboratory) for lending us a DL100 memory for the area detector. R.M. was supported by a fellowship from the Federation of European Biochemical Societies (FEBS).

9 November 1987; accepted 18 February 1988

Absence of TGF-β Receptors and Growth Inhibitory Responses in Retinoblastoma Cells

ADI KIMCHI, XIAO-FAN WANG, ROBERT A. WEINBERG, SELA CHEIFETZ, JOAN MASSAGUÉ

The responses of retinoblastoma tumor cells and normal retinal cells to various growth inhibitory factors were examined. Whereas fetal retinal cells were highly sensitive to the antimitogenic effects of transforming growth factor β1 (TGF-β1), retinoblastoma tumor cell lines were all resistant to this factor. Binding assays and affinity labeling of these cells with radioiodinated TGF-β1 revealed that the cells did not have TGF-β receptors. The retinoblastoma cells lacked the three affinity-labeled proteins of 65, 95, and 300 kilodaltons typically seen in human cell lines and thus differed from normal retinal cells and from other types of neuroectodermal tumors that display the normal pattern of receptors. Loss of TGF-β receptors, which is a rare event among tumor cells, may represent one mechanism through which these cells escape from negative control and form retinoblastomas.

DURING THE PAST DECADE, substantial advances have been made in understanding the genes and proteins that act to promote normal cell growth. Aberrant forms of these genes, the oncogenes, participate in the formation of various types of tumors. Less well developed is the study of the molecular elements that act to constrain cell growth. Negative growth control depends on two types of components: signals that pass from cell to cell, often carried by diffusible molecules, and a receptor signal-transducing mechanism that enables a cell to recognize and respond appropriately to extracellular signals.

Work over the past years has provided examples of both types of components. Thus, interferons, tumor necrosis factors, and the transforming growth factors β1 and β2 (TGF-β1 and TGF-β2) are examples of secreted factors that may act physiologically to restrain normal cell proliferation after they interact with specific cell surface receptors (*1, 2*). The antimitogenic effects of these factors have been associated in some target cells with a selective reduction in expression of the c-*myc* nuclear proto-oncogene, which may be one mechanism through which the cell responds to encounters with these factors (*3*). Moreover, a genetic deregulation that led to resistance to one of these polypeptides, an autocrine interferon, disrupted the cessation of cell growth that normally occurs during terminal differentiation; this result indicated that loss of response to negative factors might in turn have an oncogenic effect on cells (*4*).

In parallel with this work, studies of hereditary and somatically induced tumors have suggested the existence of a group of genes and gene products that are normally involved in the negative regulation of cell growth, perhaps by conferring cellular responsiveness to growth inhibitory signals (*5*). The best studied example is the model of retinoblastoma, in which the homozygous loss of the RB gene function on human chromosome 13q14 appears to trigger tumor formation (*6–8*). We investigated the possibility that retinoblastoma cells have also lost the ability to respond to one or more of the well-studied growth inhibitors responsible for cessation of growth. We now report that retinoblastoma cells fail to respond to TGF-β1.

We initially examined the sensitivity of human fetal retinal cells to the antimitogenic effects of human interferons α, β, and γ, human tumor necrosis factor–α (TNF-α), and TGF-β1. Two primary retinal cell cultures were obtained by dissection of fetal eyes (14 and 21 weeks of gestation). The cultures were exposed to these factors during the exponential phase of their growth. Highly purified preparations of the various growth inhibitors (*9*) were added at increasing concentrations to subconfluent monolayers of the retinal cells and tested for their effects on DNA synthesis and on cell number.

Neither the various interferons nor TNF-α, when applied in a wide range of concentrations (0.1 to 10 ng/ml), substantially reduced these two growth-related parameters (*10*). In contrast, human TGF-β1 reduced the growth rate of retinal cells. The dose-response curve (Fig. 1) indicates that TGF-β1 is potent in inhibiting the incorporation of [^{3}H]thymidine into DNA; the half-maximal effect is detected between 0.2 and 0.3 ng/ml (10 p*M*). When treated continuously with TGF-β1 (0.2 n*M*), these cultures remained arrested at subconfluent densities and showed no loss in cell viability even after 4 to 6 weeks of treatment. The retinal cells resumed proliferation upon removal of TGF-β1, an indication that this polypeptide exerts a reversible cytostatic effect on these cells.

In contrast to the strong sensitivity of retinal cells to TGF-β1, four retinoblastoma cell lines established from independent tumors (Y79, RB24, RB27, and Weri) were completely resistant to growth inhibition by this factor. No effect on DNA synthesis could be detected even at the highest concentrations of TGF-β1 (Fig. 1). In addition, prolonged incubation of retinoblastoma cells with TGF-β1 (0.2 n*M*) had no detectable effects on either cell number or cell morphology.

The resistance of retinoblastoma cells to

A. Kimchi, Department of Virology, Weizmann Institute of Science, Rehovot 76100, Israel.
X.-F. Wang and R. A. Weinberg, Whitehead Institute for Biomedical Research, Cambridge, MA 02142, and Department of Biology, Massachusetts Institute of Technology, Cambridge, MA 02139.
S. Cheifetz and J. Massagué, Department of Biochemistry, University of Massachusetts Medical School, Worcester, MA 01605.